Head and Neck Lymph Node Region Delineation with 3-D CT Image Registration

Chia-Chi Teng[1], Mary M. Austin-Seymour, M.D.[2], Jerry Barker, M.D.[2]
Ira J. Kalet, Ph.D.[2], Linda G. Shapiro, Ph.D.[1,4], Mark Whipple, M.D., M.S.[3]
[1]Department of Electrical Engineering
[2]Department of Radiation Oncology
[3]Department of Otolaryngology-Head and Neck Surgery
[4]Department of Computer Science
University of Washington, Seattle, WA

Abstract

The success of radiation therapy depends critically on accurately delineating the target volume, which is the region of known or suspected disease in a patient. Methods that can compute a contour set defining a target volume on a set of patient images will contribute greatly to the success of radiation therapy and dramatically reduce the workload of radiation oncologists, who currently draw the target by hand on the images using simple computer drawing tools. The most challenging part of this process is to estimate where there is microscopic spread of disease. We are developing methods for automatically selecting and adapting standardized regions of tumor spread based on the location of lymph nodes in a standard or reference case, together with image registration techniques. The best available image registration techniques (deformable transformations computed using "mutual information" optimization) appear promising but will need to be supplemented by anatomic knowledge-based methods to achieve a clinically acceptable match.

INTRODUCTION

With the development of conformal radiation therapy in the field of Radiation Oncology, it is now possible to conform a high dose of radiation to irregular target (tumor) volumes while restricting dose to the surrounding sensitive structures. However, the success of this strategy depends on knowing the exact extent of the target volume in each patient. Radiation oncologists have adopted definitions for the various components of the target volume, in order to achieve some uniformity and facilitate the conduct of interinstitutional clinical trials.[1, 2] The Gross Target Volume (GTV) is the visible and palpable tumor mass. Although it can usually be seen on images (CT and MR), it is normally not easy to automatically identify with existing image processing techniques. To date it is still usually hand drawn by clinicians using a computer drawing software tool. The Clinical Target Volume (CTV) includes the locations of microscopic local and regional spread, which usually means the GTV plus the lymph node regions around it. Microscopic disease cannot currently be imaged by any existing technique. Even the nodes themselves are often hard to identify in the images. The task of delineating these nodal regions, which is also usually done by the clinicians, is quite time consuming. Clinicians often elect to perform less aggressive, non-conforming treatment, because they do not have the time to draw the outlines of the nodal regions and CTV, even if they are confident of which node groups are likely to have disease to treat.

Image registration tools, that match different kinds of images on the same patient, e.g. CT to MR or PET, have been effective in assisting physicians to decide what regions to treat, but the actual contours still have to be drawn manually. We hypothesize that a reference model, with images and standard node groups (regions) predrawn, can be mapped to a patient to automatically define for that patient the locations of the nodal regions. This is a more challenging problem for image registration, since it involves matching between two different instances of human anatomy, rather than two images of the same anatomy.

The work we report here was conducted using the Prism radiation therapy planning system[3] not only to take advantage of the Prism drawing tools, but also to eventually be able to test the method with a series of clinical cases, and ultimately to put it into direct clinical use if it is successful.

NODAL REGION REFERENCE MODEL

Som et. al.[4, 5] undertook a study to create an imaging-based classification for the lymph nodes of the neck that can be accepted by clinicians and easily used by radiologists. Imaging anatomic landmarks were chosen to create a consistent nodal classification similar to the clinically based classifications. Radiologists must be able to identify the pertinent anatomic landmarks,

such as the bottom of the hyoid bone, the back edge of the submandibular gland, and the back edge of the sternocleidomastoid muscle. We chose a patient to serve as a reference model for creating the standard regions. At this stage the reference model is an arbitrary data set. In the course of this work, we expect to determine criteria for an optimal reference model.

We used Prism to create a series of contoured volumes representing the nodal regions on the reference model. With the Prism volume editor, we created 2-D contours for all the nodal levels on each relevant axial image. Hence the nodal regions are defined as a series of 2-D contours in the 3-D space. Figure 1 shows one of the axial images with contours of the level IA, IB, II, and V nodal regions.

IMAGE REGISTRATION ALGORITHM

Image registration is a process of finding a geometric transformation **g** between two sets of images, which maps a point **x** in one image-based coordinate system to **g(x)** in the other. By assuming the anatomy has similar characteristics between a specific patient and a reference person, we can transform a region from the reference image set to the patient image set.

The algorithm and implementation we employed was developed by Mattes and Haynor[6] for registering one patient's PET and CT image data. We adapt it for registering CT images of two different persons.

To align the patient image with the transformed reference image, we find the set of transformation parameters μ that maximizes[6] an image similarity function S:

$$\mu_{\text{optimal}} = \text{argmax}_{\mu} S(\mu) \tag{1}$$

The algorithm uses mutual information to measure the similarity (or discrepancy). Mutual information is an entropy-based measurement of image alignment derived from probabilistic measures of image intensity values.[7, 8, 9] It is calculated by estimating the marginal and joint probability distribution (histogram) of the intensity values of the test and reference images.

The joint probability distribution of the test image (f_T) and the reference image ($f_R \circ \mathbf{g}$) is calculated using the Parzen window density estimation[10] and is given by:

$$\begin{aligned} p(l,k|\mu) &= \alpha \sum_{\mathbf{x}\in V} \gamma(k - \frac{f_R(\mathbf{x}) - f_R^0}{\Delta b_R}) \\ &\quad \times \beta(l - \frac{f_T(\mathbf{g}(\mathbf{x}|\mu)) - f_T^0}{\Delta b_T}) \end{aligned} \tag{2}$$

where k, l are the indices of the probability distributions of the reference and test images corresponding to the intensity values, α is a normalization factor to ensure $\sum p(l,k) = 1$, γ is the zero-ordered spline Parzen window, and β is the cubic spline Parzen window. The image intensity values are normalized by the minimum intensity value, f_R^0 or f_T^0, and the intensity range of the histogram bins, Δb_R or Δb_T.

The marginal probability for the test image is computed from the joint probability distribution equation (2),

$$p_T(l|\mu) = \sum_k p(l,k|\mu) \tag{3}$$

The marginal probability for the reference image is independent of the transformation parameters, and can be computed as:

$$p_R(k) = \alpha \sum_{\mathbf{x}\in V} \gamma(l - \frac{f_R(\mathbf{x}) - f_R^0}{\Delta b_R}) \tag{4}$$

The negative of the mutual information between the test and reference images is used as the image discrepancy measure, which can be expressed as function of the transformation parameter vector μ and computed with equations (2), (3), and (4)[10]:

$$S(\mu) = -\sum_l \sum_k p(l,k|\mu) \log \frac{p(l,k|\mu)}{p_T(l|\mu) p_R(k)} \tag{5}$$

B-spline bases are used to represent an image to make it a continuous function $f(\mathbf{x})$ for better interpolation and sampling results. Values of $f(\mathbf{x})$ for non-integer $\mathbf{x}$ can be interpolated with the samples $f_i = f(\mathbf{x}_i), \mathbf{x}_i \in V$ by[6, 10]:

$$f(\mathbf{x}) = \sum_i c_i \beta(\mathbf{x} - \mathbf{x}_i) \tag{6}$$

The expansion coefficients c_i of the basis are computed from the f_i with a recursive filtering algorithm.[11] The cubic B-spline window β has arguments

$$\beta(x) = \begin{cases} \frac{1}{6}(4 - 6x^2 + 3|x|^3) & 0 \le |x| < 1 \\ \frac{1}{6}(8 - 12|x| + 6x^2 - |x|^3) & 1 \le |x| < 2 \\ 0 & 2 \le |x| \end{cases}$$

The transformation of a point $\mathbf{x} = [x, y, z]^T$ in the reference image coordinates to the test image coordinate is defined by a 3×3 homogeneous rotation matrix **R**, a 3-element transformation vector **T** and a deformation term $\mathbf{D}(\mathbf{x}|\delta)$[6]:

$$\mathbf{g}(\mathbf{x}|\mu) = \mathbf{R}(\mathbf{x} - \mathbf{x}_C) - \mathbf{T}(\mathbf{x} - \mathbf{x}_C) + \mathbf{D}(\mathbf{x}|\delta) \tag{7}$$

where $\mathbf{x}_C$ is the center of the reference volume.

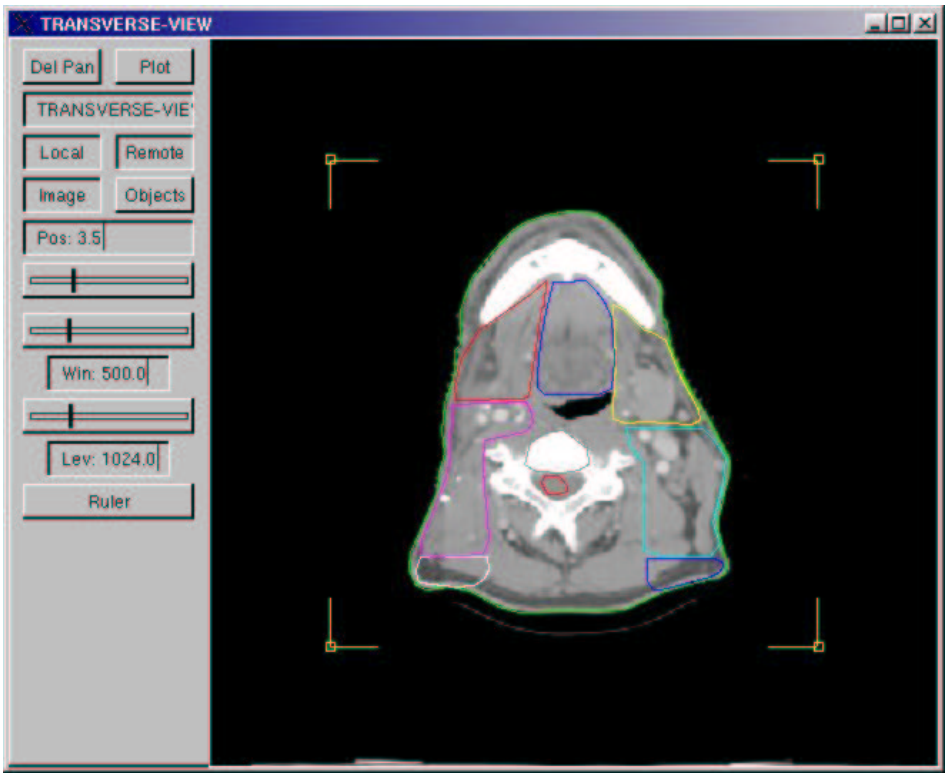

Figure 1: Nodal region contours of a reference model.

A rigid body transformation defined by **R** and **T** was first calculated, and it was used as the initial transformation for the deformation process. The deformation term $\mathbf{D}(\mathbf{x}|\delta)$ gives an x-, y-, and z- offset for each given **x**. The deformation parameters were computed at a lower resolution by choosing a grid of initially evenly spaced control points, each of which is associated with a 3-element deformation coefficient δ, describing the x-, y-, and z-components of the deformation. Hence the transformation parameter vector μ becomes[6]:

$$\mu = \{\gamma, \theta, \phi, t_x, t_y, t_z; \delta_j\} \tag{8}$$

where $\{\gamma, \theta, \phi\}$ are the roll-pitch-yaw Euler angles of **R**, $[t_x, t_y, t_z]^T$ is **T**, and δ_j is the set of the deformation coefficients, j being the index of the control points.

EXPERIMENT AND RESULTS

The reference images and test images are CT scans performed at the University of Washington Medical Center using a General Electric CT scanner. The bed and immobilization device were automatically removed from the images using thresholding and connected component operators, before the images were used for the image registration step.

Figure 2 shows a CT image from a test patient image set. Figure 3 shows an image from the transformed test image set after it was transformed to the reference space with the transformation parameters resulting from the image registration process. Figure 4 shows the reference image corresponding to the same z-plane as Figure 3.

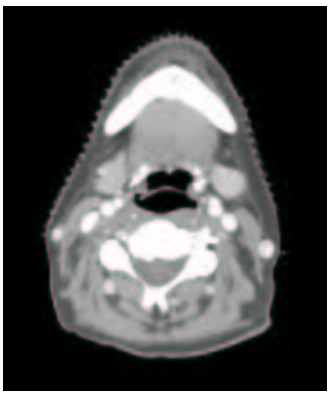

Figure 2: Test image.

The reference nodal region contours were treated as sets of 3-D points. Each point **x** was input to the function **g** in Equation (7). Then the transformed points were used to reconstruct the contours in the test image space.

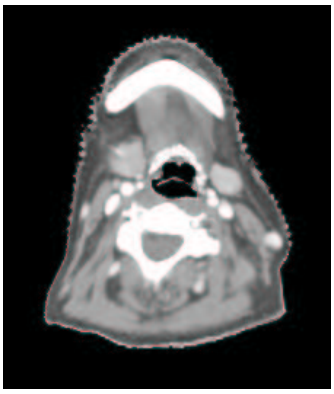

Figure 3: Test image transformed to reference space.

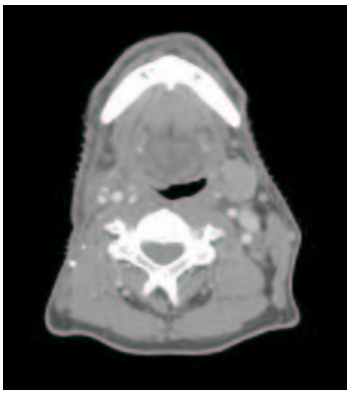

Figure 4: Reference image.

Figure 5 shows the transformed reference contours of the level IA, IB, II, and V nodal regions on a test patient axial slice. The model shown in Figure 1 was used as the reference.

DISCUSSION AND CONCLUSION

A qualitative assessment of the generated contours was made by the radiation oncologist authors (MAS and JB). While the alignment of the transformed contours on the test image are close enough to suggest the technique has promise, the results do not conform to clinical criteria. The regions an oncologist would draw on the test image will have borders that closely follow prominent anatomic objects such as bone and prominent muscles.

One problem is that the initial (rigid body) transformation for the deformation process is not sufficient for test images whose anatomy is not close to the reference model. Since this image registration method is non-landmark based, it can be very difficult to come up with a good transformation if the anatomy of the test and reference images does not overlap in the initial transformation, or is not at least in close proximity.

One potential solution is to combine the procedure with some landmark matching to create a better initial transformation for the deformation. Some image processing operations would be performed on both reference and test images to find easily identifiable landmarks and incorporate them into the initial transformation. Another approach is to provide a set of reference models instead of just one, and choose the closest one to the current patient image set.

Future work

We will first try to improve the results by incorporating landmark based initialization to work with the deformation based on mutual information. The particular landmarks that are most useful may depend on the tumor site. We will experiment with multiple reference models, including clinical patient data with different anatomical characteristics and also the image data from the Visible Human Project.[12] We will analyze the results to study the effects of the different characteristics.

We plan to integrate this work with The Digital Anatomist Foundational Model[13] knowledge-base to add the symbolic definitions of the nodal regions and their relationship to other anatomy. This will allow us to study ways to represent anatomical regions and their attributes in a knowledge-based environment.

This work will be integrated with the Prism[3] radiation therapy planning system so that it can be evaluated in a clinical setting and a broader evaluation can be perform by more clinicians on more cases.

Acknowledgments

This work was partially supported by National Institutes of Health grant LM06822 from the National Library of Medicine. Thanks also to David Haynor and David Mattes for assistance in understanding and using their programs to run the test case described in this paper.

References

1. International Commission on Radiation Units and Measurements . Prescribing, Recording and Reporting Photon Beam Therapy. Bethesda, MD, International Commission on Radiation Units and Measurements, 1993. Report 50.

2. International Commission on Radiation Units and Measurements . Prescribing, Recording and Reporting Photon Beam Therapy (Supplement to ICRU Report 50). Bethesda, MD, International Commission on Radiation Units and Measurements, 1999. Report 62.

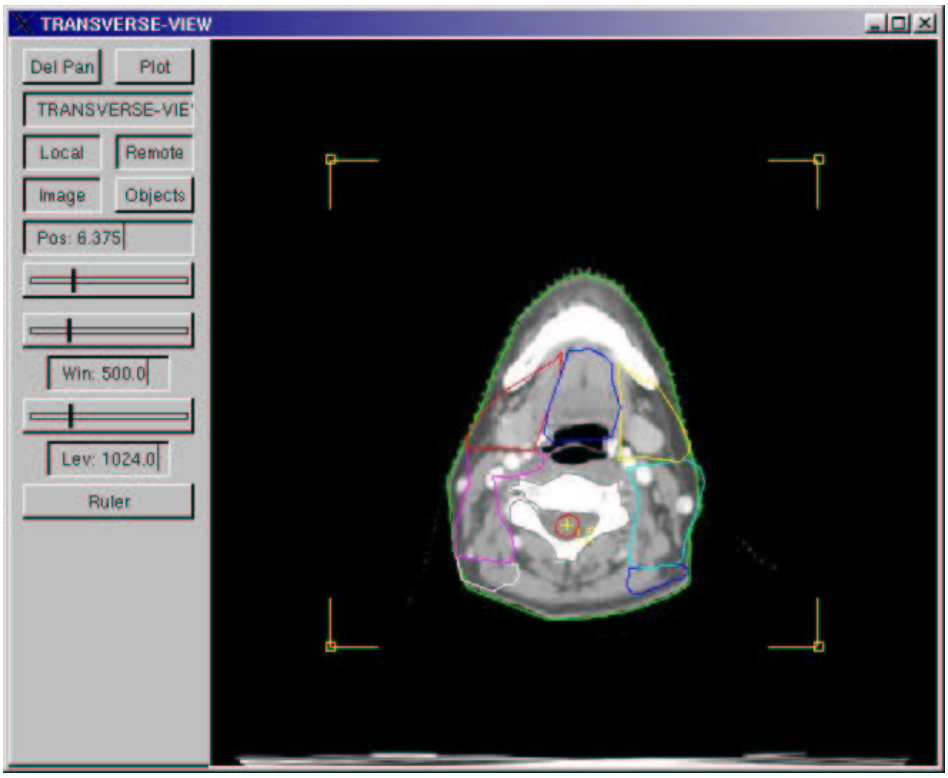

Figure 5: Nodal region contours on the test data.

3. Kalet IJ, Jacky JP, Austin-Seymour MM, Hummel SM, Sullivan KJ, Unger JM. Prism: A new approach to radiotherapy planning software. International Journal of Radiation Oncology, Biology and Physics 36:451–461, 1996.

4. Som PM, Curtin HD, Mancuso A. An imaging-based classification for the cervical nodes designed as an adjunt to recent clinical based nodal classification. Arch Otolaryngol Head Neck Surg 125:388–396, April 1999.

5. Som PM, Curtin HD, Mancuso A. Imaging-based classification for evaluation of neck metastatic adenophy. American Journal of Roentgenology 174, March 2000.

6. Mattes D, Haynor DR, Vesselle H, Lewellen TK, Eubank W. Nonrigid multimodality image registration. in Sonka M, Hanson KM, (eds), Proceedings of the SPIE Conference on Medical Imaging 2001: Image Processing. 2001.

7. Studholme C, Hill DLG, Hawkes DJ. An overlap invariant entropy measure of 3d medical image alignment. Pattern Recognition 32:71–86, 1999.

8. Maes F, Collignon A, Vandermeulen D, Marchal G, Suetens P. Multimodality image registration by maximization of mutual information. IEEE Transactions on Medical Imaging 16:187–198, 1997.

9. Viola P, Wells III WM. Alignment by maximization of mutual information. International Journal of Computer Vision 24:137–154, 1997.

10. Thevenaz P, Unser M. Spline pyramids for intermodal image registration using mutual information. Proceeding of the SPIE 3169:236–247, 1997.

11. Unser M, Aldroubi A, Eden M. Fast B-spline transforms for continuous image representation and interpolation. IEEE Transactions on Pattern Analysis and Machine Intelligence 13:277–285, March 1991.

12. National Library of Medicine . Visible human project. RFP NLM-90-114/SLC, June 1990.

13. Rosse C, Shapiro LG, Brinkley JF. The digital anatomist foundational model: Principles for defining and structuring its concept domain. in Proceedings of the Americal Medical Informatics Association (AMIA) Fall Symposium. 1998:820–824.